# BACK ANALYSES OF TIME-DEPENDENT DISPLACEMENT AT THE TROJANE TUNNEL CONSTRUCTION

JAKOB LIKAR

**about the author**

Jakob Likar
University of Ljubljana,
Faculty of Natural Sciences and Engineering
Aškerčeva 12, 1000 Ljubljana, Slovenija

**Abstract**

*The 2,900-metre double tube tunnel of Trojane forms part of the highway section between Celje and Ljubljana and part of the highway road system connecting Lendava and Koper with adjacent roads. The construction of this section, which is of special importance for the Republic Slovenia, has been going on for almost ten years.*

*The highway near Trojane, where the tunnel is located, lies on a hilly terrain composed of Permian-carboniferous rocks, which are tectonically badly damaged in some places and marked with broad fault zones, containing tectonically remoulded soil of low strength in terms of deformability properties. Even though the amount of waters coming from the hills during the excavation of the tunnel was relatively small, this water, in combination with extremely damaged weak rock caused the increase of deformations at the construction site.*

*Geological and geotechnical surveying with geometric monitoring and the analyses of stress and deformation changes in the surrounding rocks and support elements were critical in assessing the actual weak-rock conditions during the course of construction. Since the analyses of deformation processes, which had been modelled with PLAXIS 3D TUNNEL PROGRAM, showed great impact on permanent stability of the tunnel, special care was paid to rheological changes in the surrounding rocks and combined in-built support elements.*

*3D back analyses with SOFT-SOIL-CREEP (SSC) constitutive model, which takes into account rheological phenomena, were carried out. The calculations of primary and secondary stresses and deformations were made for two characteristic areas and determined on the basis of realistic geological mapping during tunnel construction. The first area represented typical rocks of the Trojane tunnel, i.e. shales and siltstone, while the second one was a tectonic zone where geological and geotechnical conditions during excavation were less favourable. The results of back analyses used provided an acceptable possibility for estimating the stress-strain variation during construction as well as an appropriate basis for analysing vertical displacements at the tunnel roof. The calculation results show good correlation with field measurements.*

**keywords**

Tunnel construction, Permian-carboniferous rocks, geological-geotechnical conditions, tunnel support, finite element method, constitutive models, back analyses, field measurement, time dependent analyses;

## 1 INTRODUCTION

The highway connecting Ljubljana and Celje is an important element of more rapid economic, social and cultural development of the region. In addition to other demanding engineering structures, several tunnels have been planned in this section: four double-tube tunnels (Ločica, Jasovnik, Podmilj and Trojane) and a single-tube tunnel in Zide, which will connect the Zasavje region with the future highway. So far, three tunnels have been finished. The Trojane and Podmilj tunnels are still under construction whilst the excavation and the construction of the primary lining have been finished.

The selection of the site for the double-tube Trojane tunnel with a 2,811-metre northern (right) tube and a 2,900-metre southern tube was made after the completion of extensive transportation and technical studies as well as environmental analyses. Geotechnical criteria were not considered to such an extent, since construction experience in similar rock conditions indicated that there was a strong demand for sophisticated construction operations. Yet, modern construction methods allow for the construction of substructures in extremely demanding geotechnical conditions, similar to those in Trojane.

The physical and mechanical properties of the rocks in the Trojane terrain, which are mainly of Permian-carboniferous origin, spread in an array of different value bands. The terrain consists of claystone, siltstone and sandstone, the rocks being primarily damaged to a different extent, which is mainly shown in their low self-bearing capacity. The rocks have more or less expressed rheological properties, depending on the content of clay minerals. For a realistic estimation of geotechnical conditions of the tunnel construction, the data on rheological sensitivity of rocks, especially on the determination of the sliding coefficient, are crucial. This aspect will be explained in more detail further on.

Figure 1 shows the situation of the construction of the Trojane tunnel that runs partially under a populated area.

- schist claystone,
- siltstone, forming a stress layer between claystone and sandstone,
- smaller patches of quartz sandstone changing into conglomerates,
- tectonic clays in the regions of shear zones and faults.

During geological ages these rocks have been exposed to tectonic activity. For this reason, the tunnel region is crossed by several shear zones of broken and tectonically remoulded rocks which have been changed into tectonic clay. In general, rock permeability is low. Smaller water inflow had appeared only in the layers of sandstone damaged by tectonic influences.

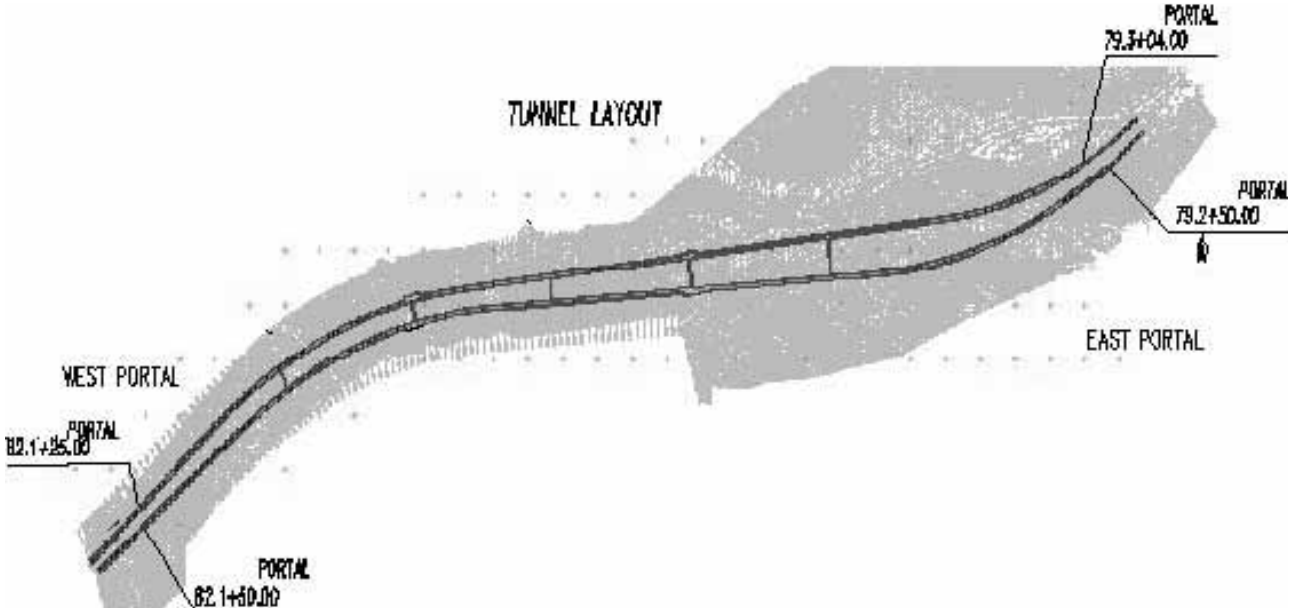


**Figure 1**. The Trojane tunnel situation.

## 2 GEOLOGICAL AND GEOTECHNICAL CONDITIONS OF THE TUNNEL

The broader Trojane region is part of the highly folded Posavje region characterized by trust structure and rock damage. The narrower Trojane region is part of the Kozjak trust or Trojane anticline. The rocks from this region are mainly composed of Permian-carboniferous clastic rocks, which appear in the layers of:

A very complex and dynamic genesis of the rocks is also reflected in large changes in the rock, which had already been proven by laboratory rock analyses before the start of the construction. The real characteristics of the rocks of this site were determined by back stability analyses of precuts and by supporting constructions in the regions of the tunnel face.

Table 1 shows the characteristic values established by back analyses.

**Table 1**. Input parameters for numeric analyses [1,2].

| | Volume mass $\gamma$ (kNm$^{-3}$) | cohesion c(kPa) | Inner friction angle $\varphi$ (°) | Elasticity module E (MPa) | Poisson ratio $\nu$ (/) | Modified creeping index $\mu^*$ (/) | Modified compression index $\lambda^*$ (/) | Modified swelling index $\kappa^*$ (/) |
|---|---|---|---|---|---|---|---|---|
| sandstone | 25 | 40 | 32 | 200 | 0.25 | / | / | / |
| siltstone | 24 | 30 | 32 | 120 | 0.33 | / | / | / |
| claystone | 24 | 30 | 26 | 65 | 0.33 | / | / | / |
| Tectonic clay | 24 | 10 | 27 | 18 | 0.33 | / | / | / |
| Tectonically remoulded claystone and siltstone | 24 | 28 | 26 | 8 | 0.33 | $3.3.10^{-4}$ | $8.3.10^{-3}$ | $2.2.10^{-4}$ |
| Schist and siltstone | 24 | 25 to 30 | 27 to 28 | 10 | 0.33 | $1.5.10^{-4}$ | $9.0.10^{-3}$ | $2.0.10^{-4}$ |

## 3 TECHNOLOGY OF TUNNEL CONSTRUCTION

Geotechnical properties of the rocks and soils found in the Trojane ridge are relatively unstable, the rocks being partly highly damaged by tectonics and frequently deviating from typical average. This fact was crucial in deciding on the machinery and other equipment used in excavation and installation of the supporting elements. During the excavation, hydraulic hammers were used. Where the weak rock was sufficiently soft, a classical excavator was also used for the excavation in bench and invert.

The excavation progressed with different speed, depending on the hardness, strength and toughness of the rock. The excavation of the top heading of an area of 53m$^2$ took from 1 to 5 hours. An important aspect was regular opening of free surfaces of rock layers, so that energy consumption was held to its minimum with optimal effect.

Since the strength of the rocks was extremely low (drilling and blasting were not necessary), a stronger support needed to be built. We decided on a combined supporting system which allowed suitable reactive support pressure of the supporting system against the pressure of surrounding rocks to achieve stable rock-support system [3].

During the construction, standard supporting elements were used, e.g. shotcrete MB25, rock passive bolts (SN, IBO) with a bearing capacity of 250kN and 350kN, reinforced meshes Q189 and Q283 and steel arch supports (TH21, K24, IPE). To ensure stable conditions during the excavation, subsidiary support elements were used, as for example steel forepoling rods, a steel pipe roof, a temporary invert arch made of shotcrete, an expanded elephant foot, micro piles, fibreglass bolts, etc. The erection of main and subsidiary support elements was done with machinery, which is usually used in tunnels (Figure 2).

The supporting system and the system of excavation was adjusted to changing geological and geotechnical conditions; thus, the construction proceeded according to the results of geotechnical measurements and observations. There were frequent cases of displacement of rocks and changes over time of stress and field deformations, as well as changes of displacements of the tunnel wall.

**Figure 2**. Installing micro piles into the side of the tunnel.

In addition to the frequency of rock squeezing during the construction of the Trojane tunnel, we also observed high residual stress in the rock mass and schistose, which caused differential settling and deformation of the tunnel tube in various directions. These phenomena required additional measures, e.g. asymmetric anchoring in order to maintain stable conditions at the acceptable level. The combination of these impacts represented the most unfavourable situation in the tunnel in terms of time stabilization of the rock and the support system.

Figure 3 shows deformations in measurement profile 77, chainage 80+920, 109m below the surface of the West left (South) tunnel tube, depicting the problems of tunnel construction in anisotropic conditions in larger absolute and differential movements.

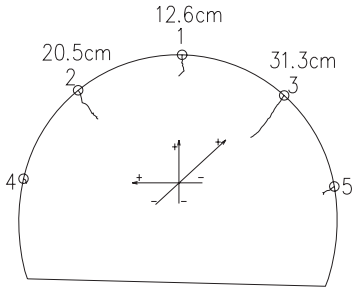


**Figure 3**. Deformations measured in metric profile 77, 109 m below the surface – West left (south) tunnel tube

## 4 STRESS AND DEFORMATION CHANGES IN THE SYSTEM ROCK-SUPPORT DURING THE EXCAVATION OF THE TUNNEL

The advancement of excavations in the rocks of low bearing capacity and in tectonically badly damaged rocks, such as claystone, siltstone and tectonic clays composing the Trojane site, was greatly influenced by changes in deformation fields occurring at the front of the excavation face and in the broader area of the tunnel. Two typical situations had to be considered: excavation in depths greater than 50m and excavation in a shallow surface layer populated on the top. In the first case the impact of the excavation at the front of the excavation face was considerably smaller and accounted for about 25% of the total vertical displacement on the surface. In the second case, the impact was more expressed at the front of the excavation face (3D or even 4D in front of the excavation face, D meaning the equivalent diameter of the excavation of the tunnel tube), which accounted for up to 50%, or in some extreme cases even 70% of the total vertical displacements.

This fact was extremely important for the estimation of the absolute scope and development of the vertical displacement of the surface above the tunnel. From the analyses and engineering interpretations so far it was

EAST SIDE

WEST SIDE

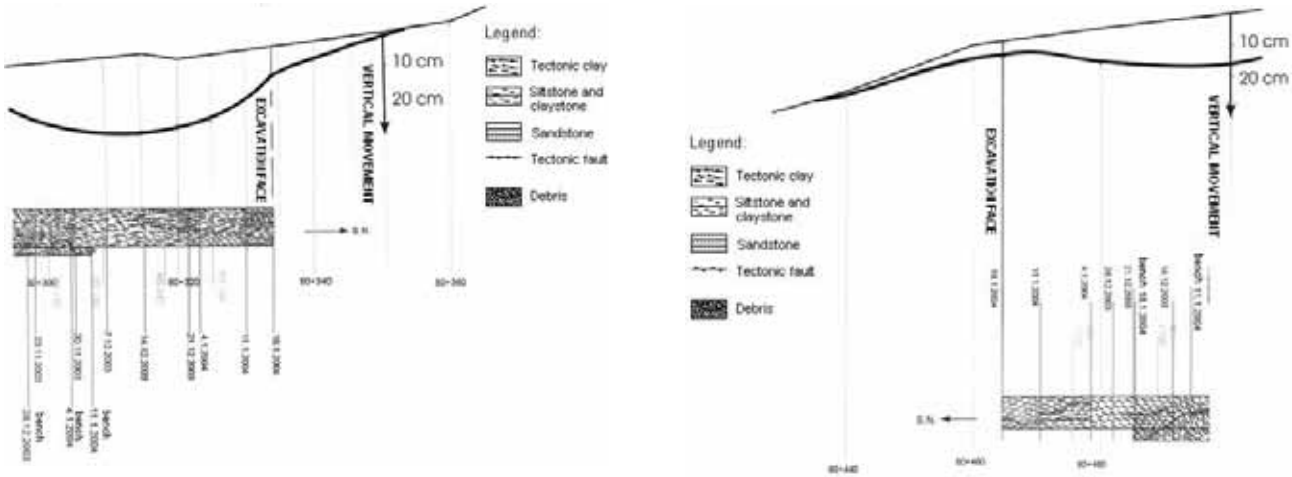


**Figure 4**. Measured vertical displacements on the surface above the left tunnel tube – eastern and western side.

possible to determine quite accurately the content of clay components in the rocks with low-bearing capacity which had a significant impact on the course of development of deformations. This was an important piece of information to predict possible changes in a long run.

Figure 4 shows vertical displacements on the surface in both cases.

# 5 TIME DEPENDENT ROCK DEFORMATION PROCESSES IN THE SUPPORTING SYSTEM

In constructing tunnels in low-bearing capacity rocks it is important to construct supporting elements after each excavation step. The elements need to have sufficient bearing capacity to achieve the required stability of the rock-support system. The cross cut point of the curve of the self-bearing capacity of the rock and the reaction pressure curve of the supporting system needs to be stable, and permanent static stability needs to be assured. This requirement is of great importance in building substructures in rheologically dependent rocks. To achieve permanent stability of the structure we need to provide static and time balance. Even if minimal deformations are present in correlation with the time we can expect an increase of additional stress in the inner lining which represents a strong, tough support element. If deformation balance is not achieved, the worst thing to happen is the collapse of the construction [4,5]. Since the above findings are important for the assessment of real stability of structures constructed in rheologically sensitive rocks, additional back analyses have been made for some sections of the Trojane tunnel.

## 5.1 EXAMPLE OF THE APPLICATION OF 3D ANALYSES IN THE TROJANE TUNNEL

Time-dependent changes in the rocks in excavating and building the supports in the Trojane tunnel have been analysed using the software package Plaxis 3D, Tunnel 1.2, which allows for the use of several different parameters of the rock-support system.

The model of time-dependent creeping of the material (SOFT SOIL CREEP - SSC MODEL) has been developed, based on oedometric tests by which we can observe rapid development of deformations during the phase of primary consolidation followed by the second consolidation phase, which can cause the material to collapse. The model has been designed as an upgrade of one-dimensional logarithm written in increment form, taking into account the creeping of the weak rock, which can be compared to the processes in edometric tests. It has been made for 3D stress conditions based on the MCC (Modified Cam Clay) model and the concepts of high plastic materials [6].

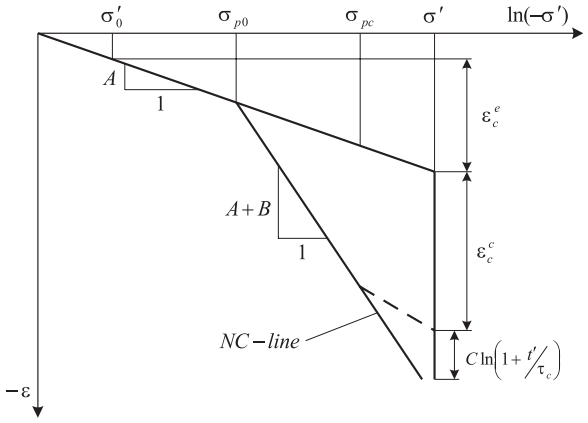


**Figure 5**. Ideal relationship between strain and stress, obtained by an oedometric test.

The following is the equation for the whole specific deformation:

$$\varepsilon = \varepsilon_c + C\ln\frac{t_c + t'}{\tau_c} = A\ln\frac{\sigma'}{\sigma'_0} + B\ln\frac{\sigma_{pc}}{\sigma_{p0}} + C\ln\frac{t_c + t'}{\tau_c} \quad (1)$$

One-dimensional creeping of the rocks can be expressed by the following equation:

$$\dot{\varepsilon} = \dot{\varepsilon}^e + \dot{\varepsilon}^c = A\frac{\dot{\sigma}'}{\sigma'} + \frac{C}{\tau}\left(\frac{\sigma'}{\sigma_p}\right)^{B/C} \quad (2)$$

where thy symbols have the following meaning:

$t$ duration of load rate
$t'$ effective creeping time
$t_c$ time from the beginning of creeping
$\tau_c$ effective time from the initial time of creeping
$\varepsilon_c$ sum of elastic and plastic specific deformation ($\varepsilon^e_c + \varepsilon^c_c$)
$\sigma'$ effective tension at the end of load rate
$\sigma'_0$ effective tension at the beginning of load rate
$\sigma_{pc}$ final pre-consolidation tension
$\sigma_{p0}$ initial pre-consolidation tension
$\sigma_p$ pre-consolidation tension
$A, B, C$ material constants
$\dot{\varepsilon}, \dot{\varepsilon}^e, \dot{\varepsilon}^c, \dot{\sigma}'$ derivations by time.

Theoretical background of the expanded model are given in the Appendix A [7].

In our case, the rocks such as tectonically remoulded claystone and siltstone, were treated as solid soils or soft rocks with low strength and deformability properties as well as other properties by which we can record stress and deformation changes during the excavation and supporting the substructure.

The following parameters have been used:

- hardness parameters, which were equal in both Mohr-Coulomb (MC) and SSC models: inner friction φ, cohesion c, dilatation angle ψ;
- basic hardness coefficients used for the model SCC were modified swelling index ($\kappa^*$), modified compression index ($\lambda^*$) and modified creeping index ($\mu^*$);
- additional parameters e.g. Poisson ratio during the de-stressing and re-stressing ($\nu_{ur}$), inclination of the critical condition line (M) and coefficient between primary and horizontal and vertical stress in normally consolidated clays ($K^{NC}_o$). In principle, the basic hardness coefficient can be determined from the curves of oedometric tests, using the following equation:

$$\kappa^* = 3A(1-\nu_{ur})/(1+\nu_{ur}) \quad (3)$$

$$\lambda^* = C_c/(2.3(1+e_o)) \quad (4)$$

$$A = C_s/(2.3(1+e_o)) \quad (5)$$

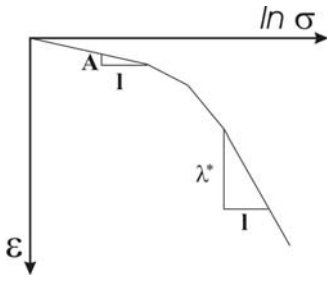


**Figure 6a**: Correlation between stress and strain logarithm.

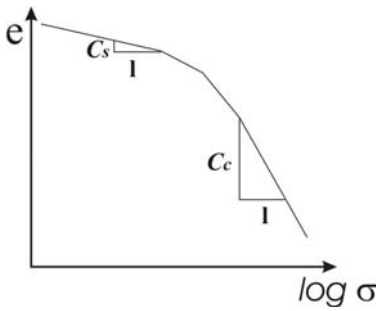


**Figure 6b**: Correlation between stress logarithm and pore ratio.

$$\mu^* = \Delta\varepsilon/(\Delta \ln t) = C_\alpha/(2.3(1+e_o)) \quad (6)$$

$$C_\alpha = \Delta e/(\Delta \log t) \quad (7)$$

In the above equations the symbols have the following meanings:

$e_o$ = initial pore ratio, e = pore ratio, ln t = natural time logarithm, log t = binary time logarithm, ε = specific axial strain.

Based on the comparisons between the calculated and measured values, the following recommendations can be applied:

$$\kappa^* = \lambda^*/5 \text{ do } \lambda^*/15 \quad (8)$$

$$\mu^* = \lambda^*/15 \text{ do } \lambda^*/30 \quad (9)$$

In the given case Poisson coefficient $\nu_{ur}$ is determined by the ratio:

$$\Delta\sigma_{xx}/\Delta\sigma_{yy} = \nu_{ur}/(1-\nu_{ur}) \quad (10)$$

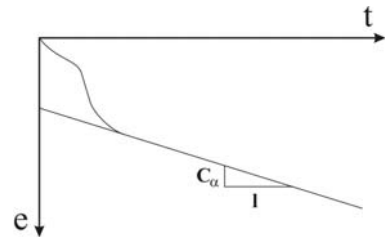


**Figure 7a**. Correlation between time and pore ratio.

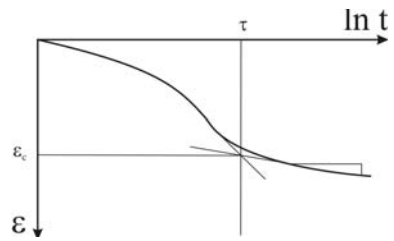


**Figure 7b**. Correlation between time logarithm and strain.

A low value of the Poisson ratio $\nu_{ur,}$ which is between 0.1 and 0.2 (the set value being 0.15), means that during the phase of de-stress the horizontal stress is considerably less diminished than the vertical stress, which means that the ratio between horizontal stress $\sigma_{xx}$ and vertical stress $\sigma_{yy}$ is increased. This is typical of preconsolidated materials [7] or of those weak rock regions where horizontal primary stresses are larger than the vertical ones which are the result of the gravity field activity.

To calculate the ratio between the primary horizontal and vertical stress in normally consolidated materials, the application of the Jaky equation is recommended [6]:

$$\sigma_{xx} = (1\text{-}\sin\varphi)\sigma_{yy,} = K_o^{NC}\sigma_{yy} \quad (11)$$

$K_o^{NC}$ is a parameter which can be adapted. Based on this correlation, the following equation has been derived for parameter M [7]:

$$M = \sqrt[3]{\frac{(1-K_o^{NC})^2}{(1-2K_o^{NC})^2} + \frac{(1-K_o^{NC})(1-2\nu_{ur})(\lambda^*/\kappa^* - 1)}{(1-2K_o^{NC})(1-2\nu_{ur})(\lambda^*/\kappa^*) - (1-K_o^{NC})(1+\nu_{ur})}} \quad (12)$$

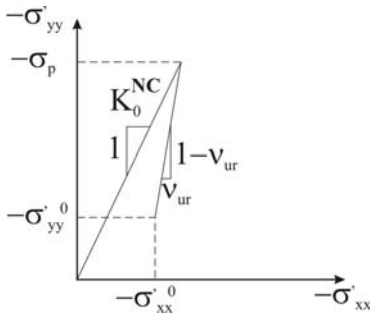


**Figure 8.** Preconsolidated stress condition achieved by primary loading and unloading of the sample.

## 6 CALCULATING SECONDARY STRESS AND DEFORMATION CONDITIONS

For calculating the secondary stress and deformation conditions we used the software package PLAXIS 3D which allowed for making the simulation of the excavation of the tunnel tube and simultaneous supporting with support elements, as for example shotcrete and rock bolts. Steel arches were not considered in calculations since they served only for providing local stability conditions and additional reinforcement of the primary lining. Several zones have been analysed in order to find out and test the possibility of real assessment made by 3D analyses in the given geotechnical conditions, which are significant both in terms of the complexity of construction and in terms of meeting the requirements for minimal and allowable vertical displacements on the surface above both tunnel tubes. The expected longitudinal geological and geotechnical profile of the right (northern) tunnel tube is shown in Figure 9.

A part of geological and geotechnical interpretation of the sections analysed is shown in Figure 10 (see next page) which gives geotechnical conditions with simultaneous analysis of each step of the excavation. By determining the GSI (Geological Strength Index) [9] for both sections analysed, the elements for determining strength parameters for two types of rocks, i.e. schist and siltstone, have been given, while for low-bearing tectonically remoulded and broken schist and siltstone rocks the index is lower.

Excavation and construction of the supporting elements have been carried out successively in the top heading, the bench and the invert arch, as shown in Figure 11, which depicts the distribution of supporting elements. It also shows asymmetric anchoring in the top heading, which has been carried out on the left side of the tunnel tube in some cases and on the right side of the tube in other cases. With anchoring, it was possible to partially diminish an increased differential vertical displacement between the left and the right side of the top heading. This displacement occurs due to expressed anisotropy of the rocks and micro layers with small shear resistance combined with schist which was frequently changing.

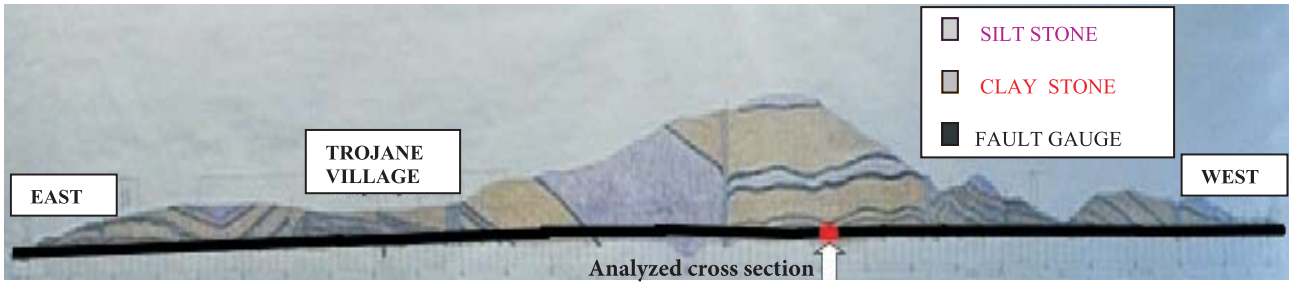


**Figure 9**. The expected longitudinal geological and geotechnical profile of the right (northern) tunnel tube.

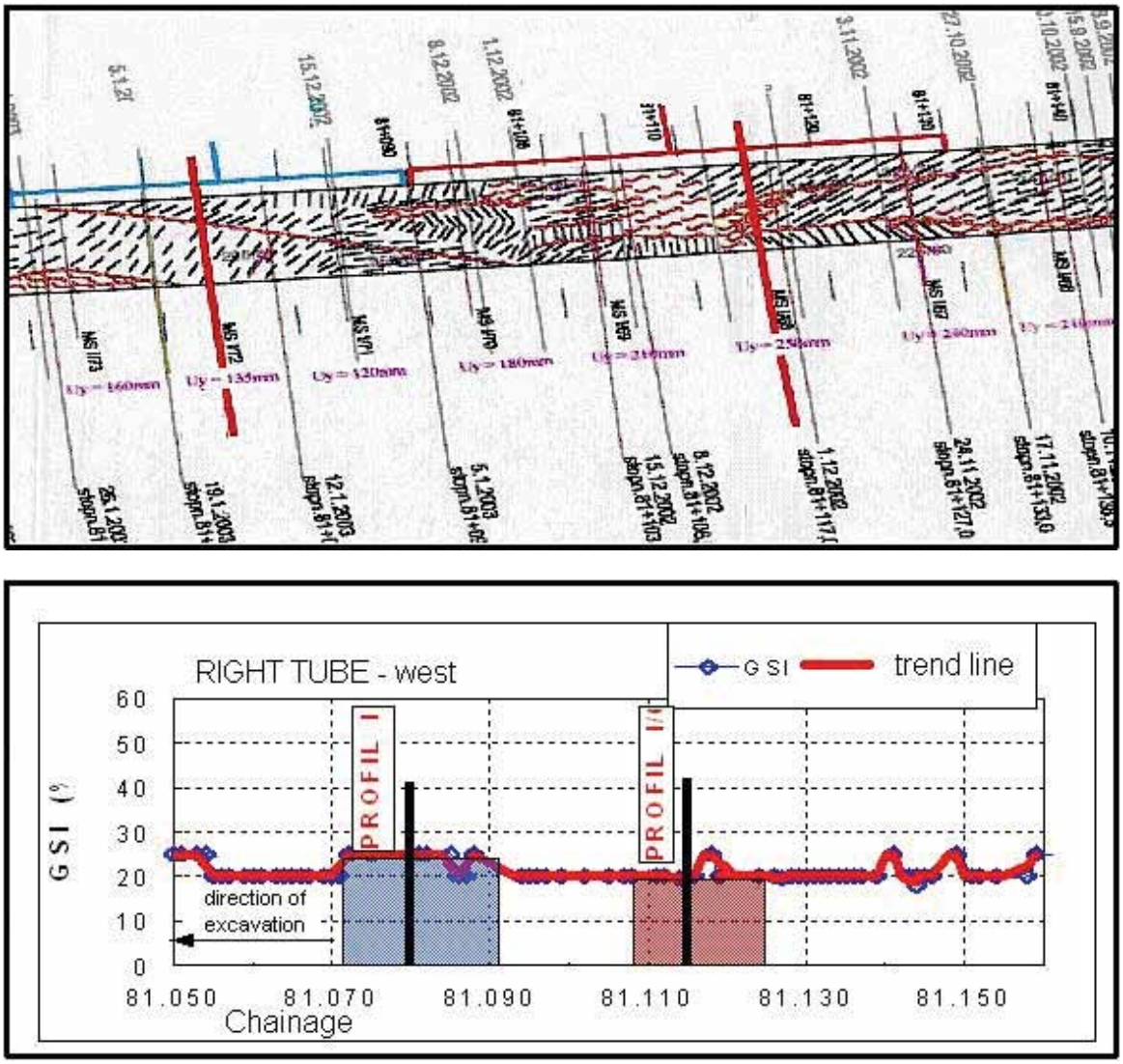


**Figure 10**. Presentation of the analysed sections.

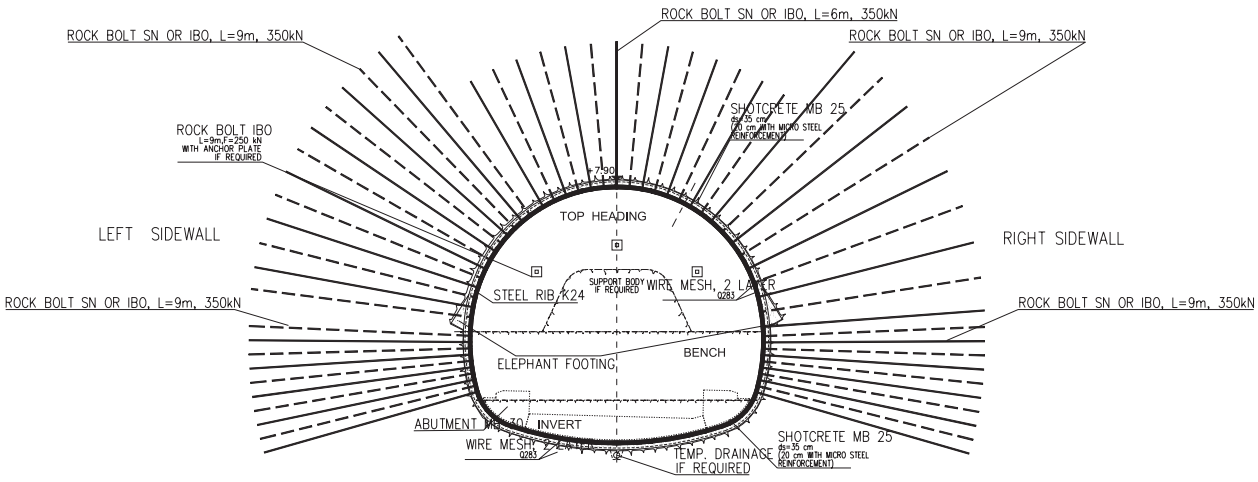


**Figure 11**. Supporting elements in the upgraded Rock Mass Type C3.

Back analyses in the sections mentioned above were designed by taking into account the deformations measured in the tunnel tube and selected measurement profiles. For basic estimation we measured the deformation in the roof point of the top heading, which was also compared with the calculated value.

Table 2 shows characteristics of primary shotcrete lining and rock bolts, while other geomechanical properties are given in Table 1. A finite element mesh was created in the space of 25m x 30m x 40m, using an axe-symmetric approach which allowed for vertical displacement in both sides and fixed nodes in the bottom of the mesh. For better simulation of the excavation process, a larger mesh would be suitable but a high capacity PC should be used. The calculations were made by taking into account the 35cm thick primary lining of shotcrete MB25 and 6m and 9m long rock bolts with bearing capacity of 350kN, and by considering excavation steps of 1m in the top heading. The simulation was carried out on a 25m section (time spent on calculations approx. 24 hours).

Figure 12 shows the procedure for advancement in the top heading, bench and in the invert arch.

The simulation of excavation of the tunnel tube was made in the following phases and time intervals:

- excavation of the face of top heading and building of primary lining – four-step excavation by 1m; duration 2 days;
- excavation of the bench and building of primary lining – two-step by 2m; duration 1 day;
- excavation and building of invert arch – one-step 4m in length; duration 1 day.

The excavation of the face was simulated in time intervals of four hours, while the building of the supporting elements was simulated in time intervals of eight hours, etc.

Since the decreasing of the deformation on a time scale is more intensive only after building the invert, this fact was also considered in calculations.

**Table 2**. Input data for primary lining (Merhar 2003).

| PRIMARY LINING | | ROCK BOLTS | |
|---|---|---|---|
| Primary lining thickness | d = 0.35m | Elastic module of steel | $E_s$ = 207000 MPa |
| Elastic module of shotcrete | $E_c$ = 10000 MPa | Rock bolt cross section | $A_b$. = $6.16.10^{-4}$ m$^2$ |
| Axial rigidity of the primary lining | EA = $8.75.10^6$ kN/m | Axial rigidity of the rock bolt | $E_sA_b$ = $1.275.10^5$ kN |
| Bending rigidity of the primary lining | EI = $8.93.10^4$ kNm$^2$ | Maximum force in the anchor | $F_{max}$ = 350kN |
| Poisson ratio | ν = 0.15 | | |

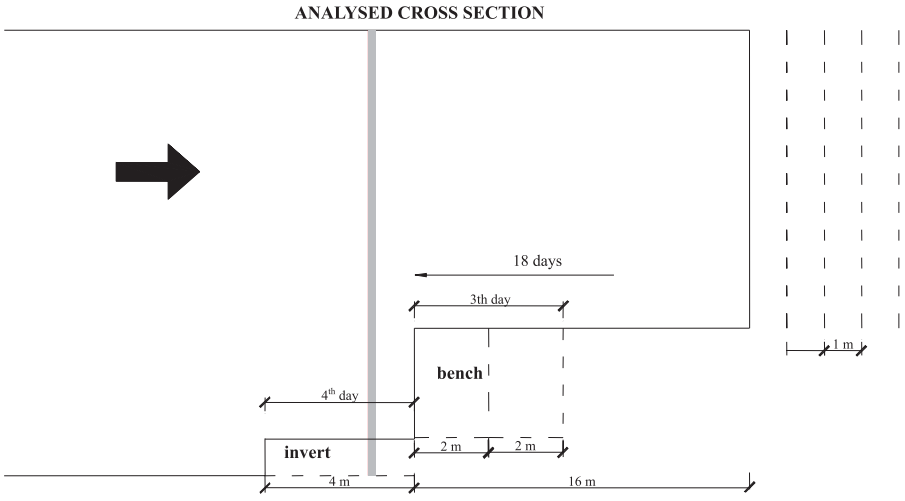


**Figure 12**. Diagram presentation of the advancement of excavation in the tunnel tube made by numeric simulation.

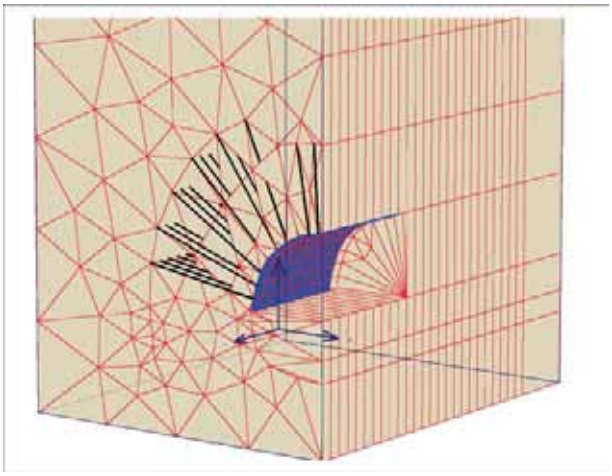

a) excavation in the top heading

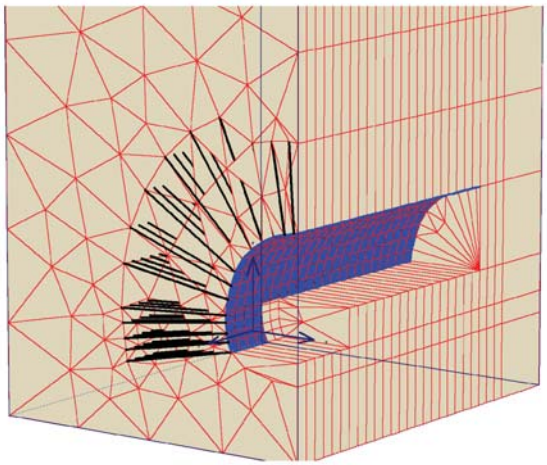

b) excavation in the bench

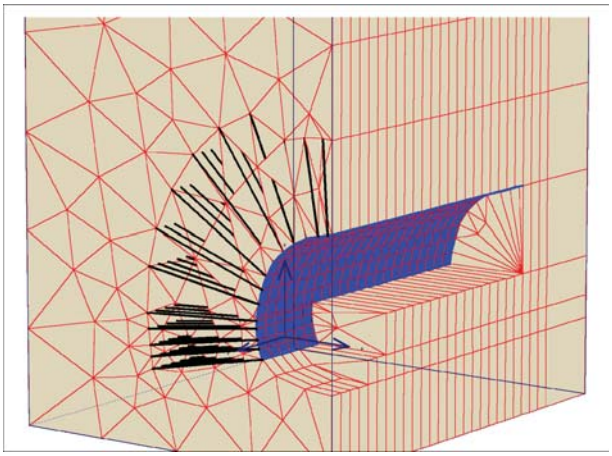

c) excavation in the invert arch

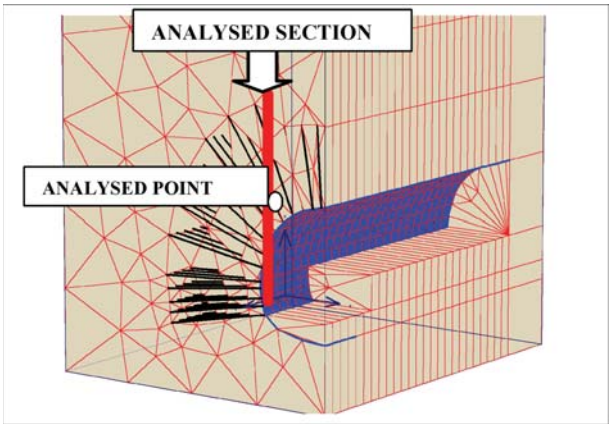


d) final situation after excavating 25m of the topheading and 6m of the bench

**Figures 13 a), b), c), and d)**. Excavation in the top heading, bench and invert arch.

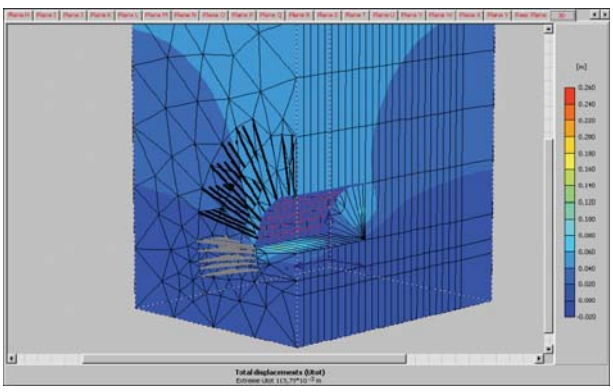

**Figure 14. a)** Deformation field after excavating 10m of the top heading; duration of the excavation 6 days.

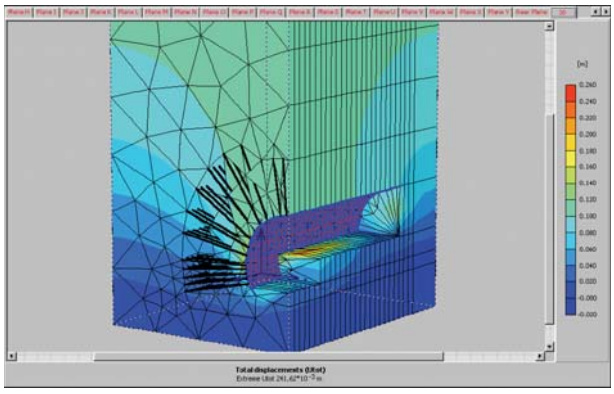

**Figure 14. b)** Deformation field after excavating 22m of the top heading and 6m of the bench; duration of excavation 25 days.

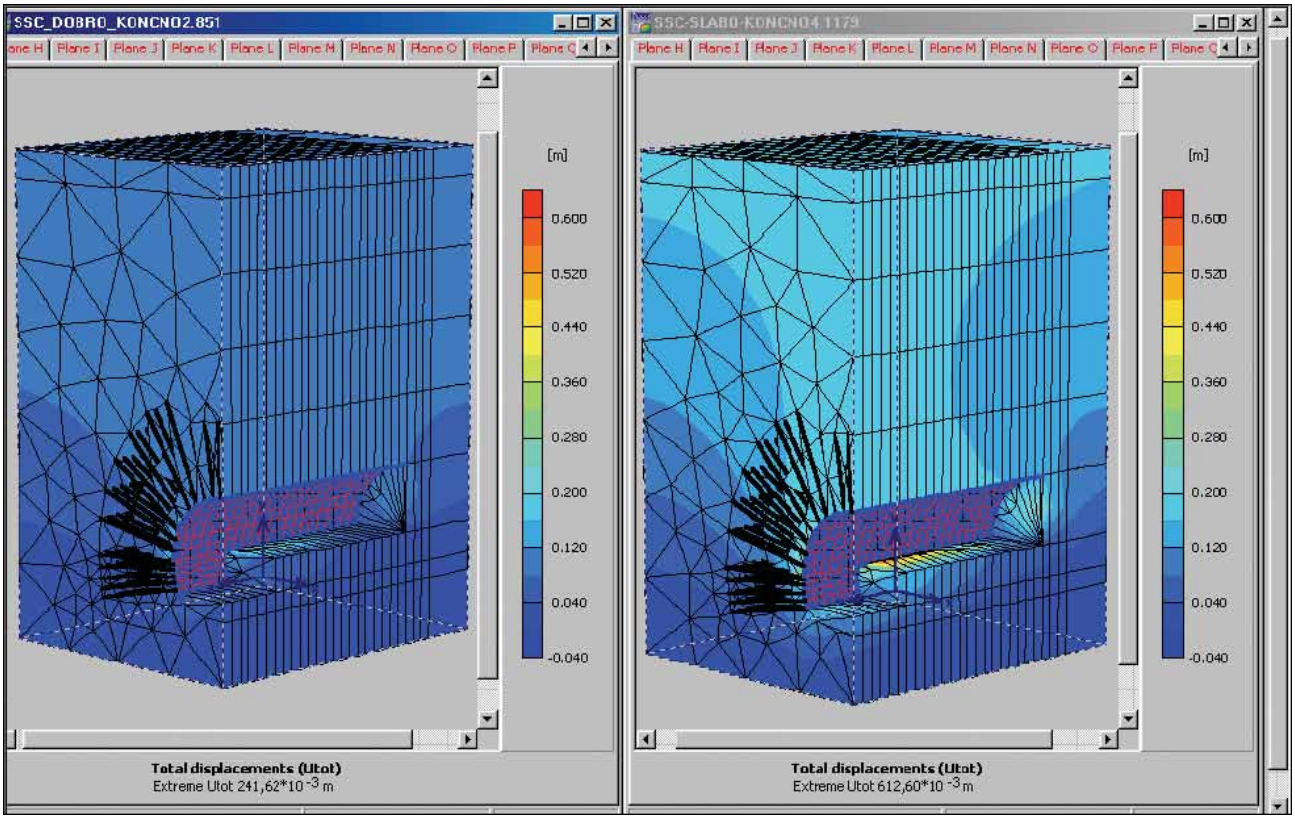


**Figure15**. Development of deformation fields for more demanding and less demanding geotechnical construction conditions.

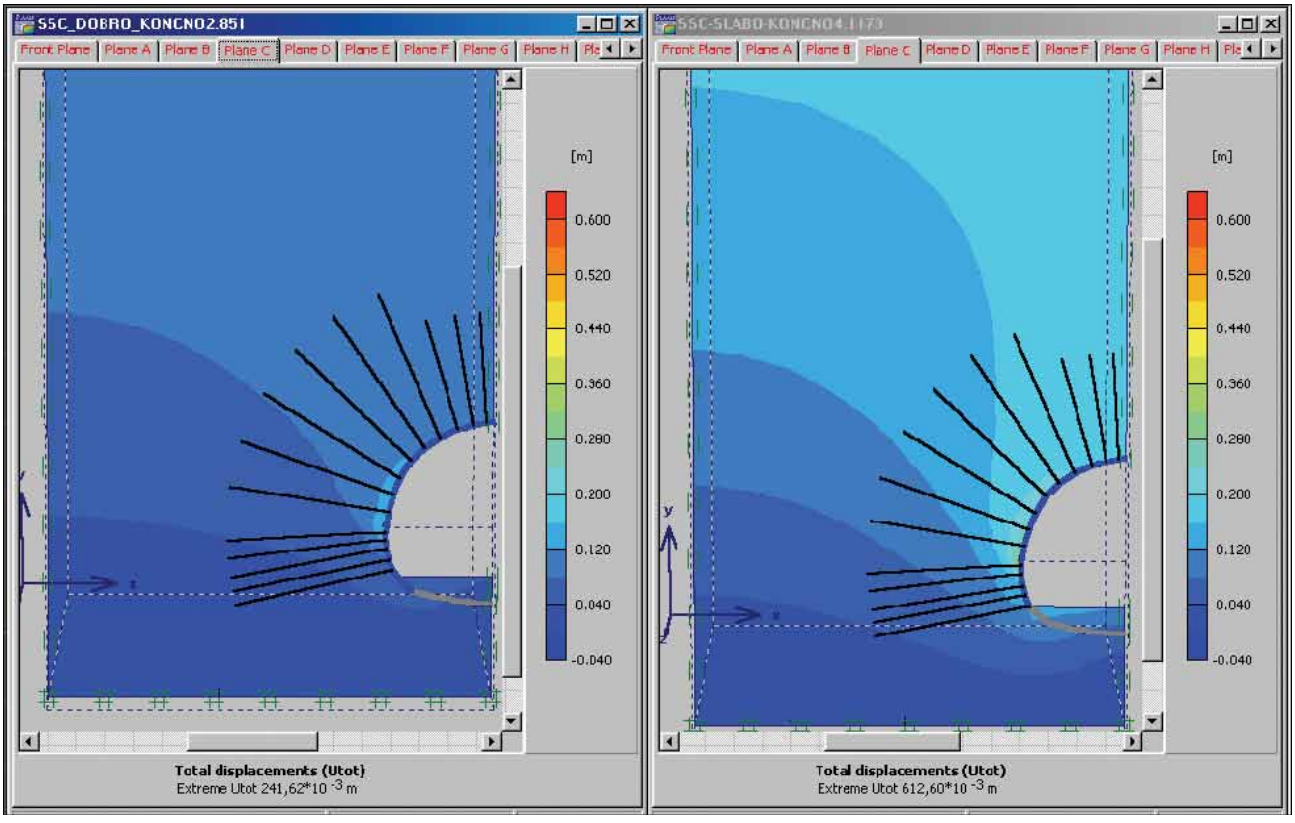


**Figure 16**. Deformation field after the excavation of the top heading and the bench in more demanding and less demanding geotechnical conditions.

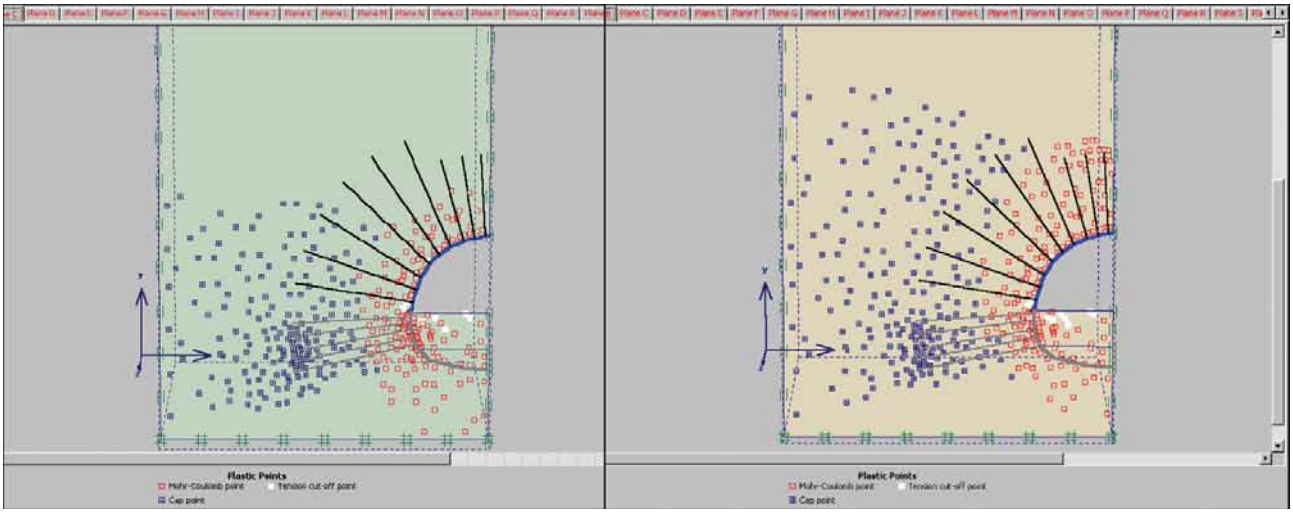


**Figure 17**. Development of a plastic region around the top heading of the tunnel tube in more demanding and less demanding geotechnical conditions.

The shape of the field is approximately the same, differences exist only in the size of deformations (from 15 cm in the ceiling of the tunnel, where the conditions are better, up to 25 cm in less favourable situations).

In both cases the deformation field which is formed in front of the face of the excavation extends into the interior under a similar angle (30° – 45°). Also, the deformations in the rock pillar in front of the excavation face are larger in more complicated geotechnical conditions, which is due to the toughness and rigidity of the impact area. In cases where the toughness of the rock pillar is exceeded, and the rock passes into a plastic area, it is necessary to stabilise the face of the excavation by using subsidiary support elements, e.g. shotcrete together with reinforced mesh and weak rock bolts.

## 7 MEASURED AND CALCULATED TIME-DEPENDENT DEFORMATION CHANGES COMPARED

Deformation and stress changes, which occurred due to the excavation and support in different geotechnical conditions, also manifested themselves in increased displacements in some cases. It has to be stressed that the possibility to manage the deformations that occurred in time was, among other things, also due to infrastructure and other facilities on the construction site. Calculations made indicated that there existed compatibility between actual occurrence and monitoring of the tunnel. This gives the analyses still greater significance and enhances the application of such analyses in similar geotechnical conditions.

The comparison between the planned and executed support measures during construction has shown that in geologically and geotechnically complex rocks it is necessary to increase the thickness of the primary shotcrete MB25 lining from 25 cm to 35 cm, to increase the bearing capacity of rock bolts from 250kN to 350kN, and to decrease the distance between the bolts to 0.85m. In some cases longer bolts, i.e. 12m, had to be built in.

## SECTION X

The analysed cross section X was selected so that the excavation was simulated beforehand in the length of 18m in the time interval of 18 days. From the presentation of the development of vertical displacements over time $U_y$ in the ceiling of the top heading, it can be seen that the displacements of 5.5cm develop in front of the excavation face in more favourable geotechnical conditions and are twice bigger in less favourable geotechnical conditions.

The comparison between the measured and the calculated time-dependent formations shows a relatively good agreement, which is a kind of evidence that the model used in the given geotechnical conditions is useful. The development of deformations over time were simulated for the period of 90 days from the time of excavation in the analysed profile and by taking into account all the required construction phases. The simulation shows that the deformation still developed after closing the ring of the inner lining, yet with expressed smaller trend towards value 0. This finding is important for the assessment of the permanent stability in case the expected

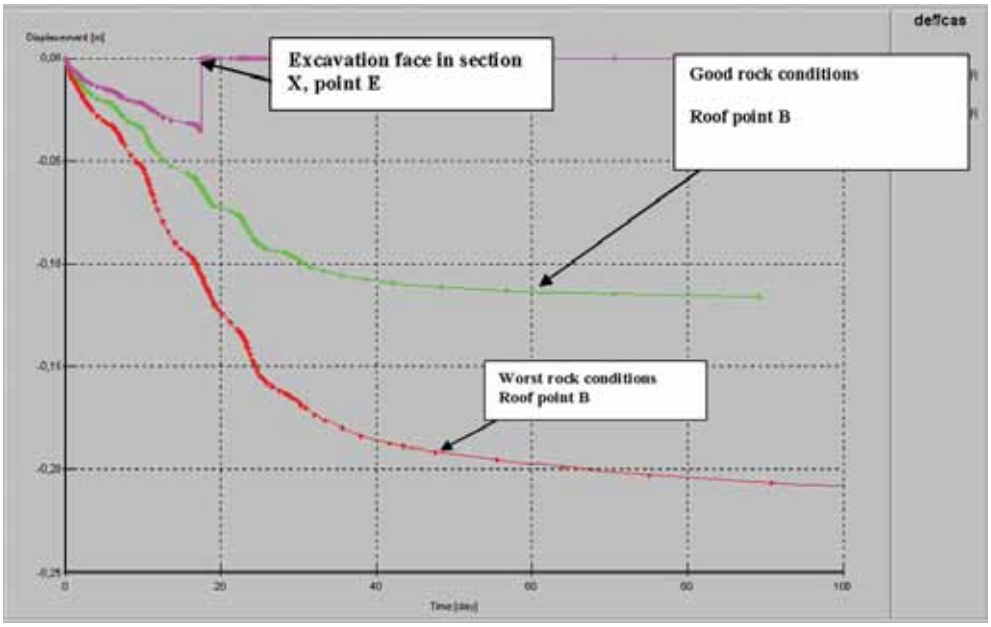


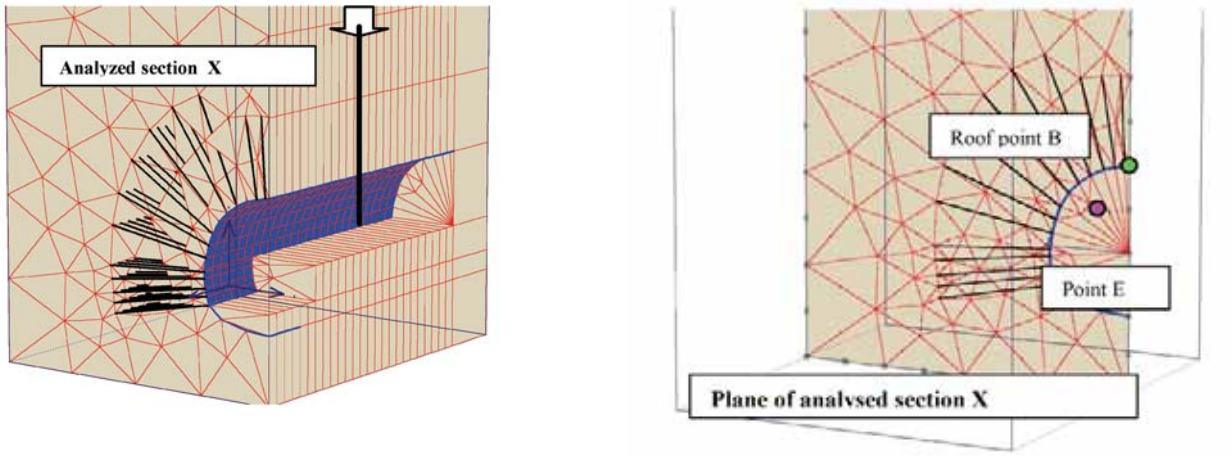


**Figure 18**. The impact of excavation in the top heading on the development of deformations in front of the excavation face.

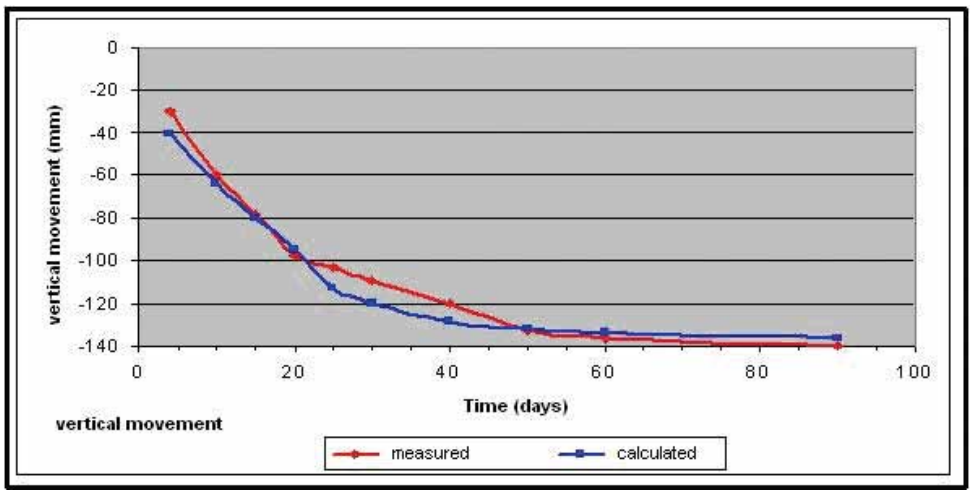


**Figure 19**. Comparison between calculated and measured displacements in the ceiling of the top heading in the analysed profile 90 days after the excavation

stagnation does not occur, so it is possible to expect an increase of additional stress in the inner lining. If the total supporting system, which consists of a primary and secondary lining and all the supporting elements, does not have a sufficient bearing capacity, it is possible to expect damages will develop over time.

## 8 SUMMARY

In building the Trojane tunnel we used a technology based on the principles of NATM (New Austrian Tunnelling Method) construction in extremely demanding geotechnical conditions. Simultaneous adaptations of the excavation method and supporting system were adjusted to geological findings and to the results of geotechnical measurements in the tunnel and on the surface.

The greatest problems in the construction were caused by primary and other forms of stress in the rocks as well as by the unfavourable position of the schist and bedding regarding the direction of the excavation. Anisotropy of the rocks and their changeability frequently demanded timely measures and the addition of supporting elements.

The instability of the excavation face and increased tension stress in the primary lining was observed during the advancement of the excavation in the west-east direction. It was necessary to ensure suitable stability conditions by weak rock bolts, reinforced meshes and thin shotcrete linings after each phase of the excavation.

The analysis of the deformation development over time was carried out using the program package 3D Plaxis and the constitutive material Soft-Soil-Creep (SSC) in real time, which allowed for a realistic simulation of the excavation while partially supporting ideal conditions.

The two sections of the tunnel analysed in more and less demanding geotechnical conditions proved the usability of the calculation method and of the treatment of deformation changes that occurred during the advancement of the excavation of the tunnel in rheologically sensitive rocks.

The applied model is suitable for prediction analyses of deformation and stress field developments over time if real input data are available. In planning the construction of substructures, this condition is difficult to accomplish in many cases. Yet, it is possible to apply back analyses during the construction works and thus determine sufficient impact parameters and carry out the necessary analyses, the results of which allow for real assessment of permanent stability of the structure in rheologically dependent rocks.

## APPENDIX A

### SPATIAL MODEL OF CREEPING IN 3D STRESS SPACE

To extend the model from planar to spatial stress condition we need to introduce stress invariants p and q, defined as:

$$p' = \frac{1}{3}\left(\sigma_1' + \sigma_2' + \sigma_3'\right) \quad \text{in}$$

$$q = \frac{1}{2}\sqrt{\left(\sigma_1 - \sigma_2\right)^2 + \left(\sigma_1 - \sigma_3\right)^2 + \left(\sigma_2 - \sigma_3\right)^2} \qquad \text{(A1)}$$

A modified Cam-clay model serves as a basis for extending the model, and describes the stress condition on the p-q plane by the help of ellipses. By invariants p and q a new defined variable is $p^{eq}$:

$$p^{eq} = p' + \frac{q}{M^2 p'} \qquad M = \frac{6\sin\varphi_{cv}}{3 - \sin\varphi_{cv}} \qquad \text{(A2)}$$

Equation (A2) is the equation of the ellipsis, which assumes $p^{eq}$ as a constant value, while parameter M gives the inclination of the critical state line (critical state line CSL). The model is shown in Figure 1A.

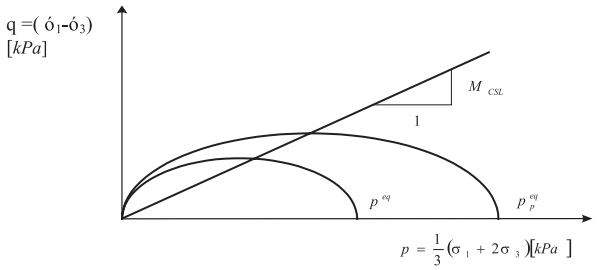


**Figure 1A**. Ellipses $p^{eq}$ in p-q plane [7].

Since this derivation is based on edometric tests, where the samples at the end of load rate are normally consolidated and where $\sigma_2 = \sigma_3 = K_0^{NC}\sigma_1$, the equations can be written as follows (A2):

$$p^{eq} = \sigma'\left[\frac{1 + 2K_0^{NC}}{3} + \frac{3\left(1 - 2K_0^{NC}\right)^2}{M^2\left(1 + 2K_0^{NC}\right)}\right] \qquad \text{(A3)}$$

$$p^{eq} = \sigma' \left[ \frac{1+2K_0^{NC}}{3} + \frac{3\left(1-2K_0^{NC}\right)^2}{M^2\left(1+2K_0^{NC}\right)} \right] \qquad \text{(A4)}$$

in which $p_p^{eq}$ 3D denotes pre-consolidation stress.

By introducing equations (A3) and (A4) into equation (A1), it is possible to omit the elastic part of deformations and to introduce a volumetric deformation instead of an axial deformation. Thus we get:

$$\dot{\varepsilon}_v^c = \frac{C}{\tau}\left(\frac{p^{eq}}{p_p^{eq}}\right)^{\frac{B}{C}} \qquad p_p^{eq} = p_{p0}^{eq} e^{\frac{\varepsilon_v^c}{B}} \qquad \text{(A5)}$$

Instead of parameters A, B and C we introduce the parameters which belong to the mechanics of critical state:

$$\kappa^* = \frac{3\left(1-\nu_{ur}\right)}{\left(1+\nu_{ur}\right)} A \qquad \lambda^* = B + \kappa^* \qquad \mu^* = C \qquad \text{(A6)}$$

The equation (A5) can be written as:

$$\dot{\varepsilon}_v^c = \frac{\mu^*}{\tau}\left(\frac{p^{eq}}{p_p^{eq}}\right)^{\frac{\lambda^*-\kappa^*}{\mu^*}} \qquad p_p^{eq} = p_{p0}^{eq} e^{\frac{\varepsilon_v^c}{\lambda^*-\kappa^*}} \qquad \text{(A7)}$$

and represents a direct extension of 1D edometric model into the spatial stress state.

In addition to the volume, it is necessary to consider the deformations in distortion stress conditions. It is necessary to record the deformations due to creeping in the form of time-dependent plastic deformations in a general form by introducing the function of plastic potential. The deformations and stresses need to be written in the form of vectors.

$$\vec{\sigma} = \left(\sigma_1, \sigma_2, \sigma_3\right)^T \qquad \vec{\varepsilon} = \left(\varepsilon_1, \varepsilon_2, \varepsilon_3\right)^T \qquad \text{(A8)}$$

The general equation for deformations is divided into the elastic and plastic part where the elastic part is derived from the Hook law, while the plastic part is determined by the equation of the plastic potential

$$\dot{\vec{\varepsilon}} = \dot{\vec{\varepsilon}}^e + \dot{\vec{\varepsilon}}^c = \vec{D}^{-1}\dot{\vec{\sigma}} + \lambda \frac{\partial Q^c}{\partial \vec{\sigma}} \qquad \text{(A9)}$$

in which the elasticity matrix and the function of plastic potential are defined as:

$$\vec{D}^{-1} = \frac{1}{E_{ur}} \begin{bmatrix} 1 & \nu_{ur} & \nu_{ur} \\ \nu_{ur} & 1 & \nu_{ur} \\ \nu_{ur} & \nu_{ur} & 1 \end{bmatrix} \qquad Q^c = p^{eq} \qquad \text{(A10)}$$

By considering all three components of the deformation, and regarding the previous equation it is possible to draw the general equation for the deformations of the plastic part.

$$\dot{\varepsilon}_v^c = \dot{\varepsilon}_1^c + \dot{\varepsilon}_2^c + \dot{\varepsilon}_3^c = \lambda\left(\frac{\partial p^{eq}}{\partial \sigma_1'} + \frac{\partial p^{eq}}{\partial \sigma_2'} + \frac{\partial p^{eq}}{\partial \sigma_3'}\right) = \lambda \frac{\partial p^{eq}}{\partial p'} = \lambda\alpha \qquad \text{(A11)}$$

It is necessary to define the mathematical model for the elastic part of deformations in the 3D stress condition. The elastic module $E_{ur}$ is written as a tangent module, dependent on the stress:

$$E_{ur} = 3\left(2-\nu_{ur}\right)K_{ur} = 3\left(2-\nu_{ur}\right)\frac{p}{\kappa^*} \qquad \text{(A12)}$$

From this equation it can be seen that the tangent module is not being introduced directly, but it is determined from the ratio between the invariant p and the modified compression module $\kappa^*$, while the Poisson ratio is introduced as a material constant. The elastic part of deformations can be written as:

$$\dot{\varepsilon}_v^e = \kappa^* \frac{\dot{p}'}{p'} \qquad \text{(A13)}$$

and integrated with time

$$\int \frac{\varepsilon_v^e}{t} dt = \int \kappa^* \frac{p'}{p'^t} dt \qquad \text{(A14)}$$

thus obtaining:

$$\varepsilon_v^e = \kappa^* \ln \frac{p'}{p_0'} \qquad \text{(A15)}$$

In the spatial model, the elastic deformations depend on the average effective stress $p'$ and not on the effective normal stress like in the 1D model. For a one-dimensional compression state, which follows the line of normal consolidation, we can draw:

$$3p_0' = \left(1+2K_0^{NC}\right)\sigma_0' \qquad \text{(A16)}$$

$$3p' = \left(1+2K_0^{NC}\right)\sigma' \qquad \text{(A17)}$$

resulting in:

$$\frac{p'}{p'_0} = \frac{p\sigma}{p\sigma'_0} \qquad \text{(A18)}$$

For the spatial model, by considering equation (18) we can draw

$$\varepsilon_v^e = \kappa^* \ln\left(\frac{\sigma'}{\sigma'_0}\right) \qquad \text{(A19)}$$

and for the 1D model the following:

$$\varepsilon_v^e = A \ln\left(\frac{\sigma'}{\sigma'_0}\right) \qquad \text{(A20)}$$

However, the analogue derivation between the 1D and 3D model is valid only for normally consolidated states, while for pre-consolidated stress states the following equation needs to be taken:

$$\frac{\dot{p}'}{p'} = \frac{1+\nu_{ur}}{1-\nu_{ur}} \frac{\kappa^*}{1+2K_0^{NC}} \frac{\dot{\sigma}'}{\sigma'} \qquad \text{(A21)}$$

meaning that:

$$\dot{\varepsilon}_v^e = \kappa^* \frac{\dot{p}'}{p'} = \frac{1+\nu_{ur}}{1-\nu_{ur}} \frac{\kappa^*}{1+2K_0} \frac{\dot{\sigma}'}{\sigma'} \qquad \text{(A22)}$$

since $K_0$ depends on the level of pre-consolidation.

Now it is possible to draw the general equation for deformations:

$$\dot{\vec{\varepsilon}} = \vec{D}^{-1} + \frac{\dot{\varepsilon}_{vc}}{\alpha} \frac{\partial p^{eq}}{\partial \vec{\sigma}} = \vec{D}^{-1} \dot{\sigma}' + \frac{\mu^*}{\alpha\tau} \left(\frac{p^{eq}}{p_p^{eq}}\right)^{\frac{\lambda^*-\kappa^*}{\mu^*}} \frac{\partial p^{eq}}{\partial \vec{\sigma}} \qquad \text{(A23)}$$

in which

$$p_p^{eq} = p_{p0}^{eq} e^{\left\{\frac{\varepsilon_v^c}{\lambda^*-\kappa^*}\right\}} \qquad \varepsilon_{vc} = \left(\lambda^* - \kappa^*\right) \ln \frac{p_p^{eq}}{p_{p0}^{eq}} \qquad \text{(A24)}$$

It is necessary to define also the plastic yield condition and the equation of yielding after the break. The criterion for SSC and MC is:

$$f = (\dot{\sigma}, c, \psi) = 0 \qquad \text{(A25)}$$

while plastic deformations are determined by the rule of yielding:

$$\dot{\vec{\varepsilon}}^p = \lambda \frac{\partial Q}{\partial \vec{\sigma}} \qquad Q = Q(\sigma, \psi). \qquad \text{(A26)}$$

## REFERENCES


[1] Vukadin, V. (2001). *Uporabnost različnih konstitutivnih modelov hribin pri analizi podpornih konstrukcij*. Magistrsko delo, Univerza v Ljubljani, Naravoslovnotehniška fakulteta.

[2] Merhar, B. (2003). *Časovno odvisne spremembe napetostno deformacijskih stanj v kamninah pri gradnji podzemnih objektov*. Magistrsko delo, Univerza v Ljubljani, Naravoslovnotehniška fakulteta.

[3] Likar, J. (2000 – 2004). *Projekt za izvredbo - PZI za predor Trojane*. IRGO Consulting, d.o.o. Ljubljana.

[4] Cristescu, N.D. (1989). *Rock rheology*. Kluwer, Dordrecht.

[5] Cristescu, N.D. and Hunsche, U. (1998). *Time effect in rock mechanics*. Wiley, Chicsester.

[6] Vermeer, P.A. and Neher, H.P. (2000). *A soft model that accounts for creep. V. Course for experienced Plaxis users*. Amsterdam.

[7] Brinkgreve, R.B. and Vermeer, P.A. (2001). *Plaxis: 3D Tunnel, Version 1*. Balkema.

[8] Šuklje, L. (1984). *Mehanika tal*. Fakulteta za arhitekturo, gradbeništvo in geodezijo, Ljubljana.

[9] Videnič, M. and Likar, J. (2002). Possibility of GSI application in permocarbonian layers. *RMZ – Materials and Geoenvironment*, vol. 49, No.4, 527-547.